

FR-3548

N R L REPORT 3548

**STUDIES OF TIME-POTENTIAL CHANGES
ON AN ELECTRODE SURFACE
DURING CURRENT INTERRUPTION**

PART I

ZINC-STEEL COUPLE IN SYNTHETIC SEA WATER

Sigmund Schuldiner and Roger E. White

October 5, 1949

Approved by:

Dr. J. C. White, Head, Electrochemistry Branch
Dr. P. Borgstrom, Superintendent, Chemistry Division
Dr. R. M. Page, Superintendent, Radio Division III



NAVAL RESEARCH LABORATORY

CAPTAIN F. R. FURTH, USN, DIRECTOR

WASHINGTON, D.C.

Distribution Unlimited

Approved for
Public Release

DISTRIBUTION

CNO	1
ONR Attn: Code 470	1
Supt., USNPGS	1
Dir., USNEL	2
CDR, USNOTS Attn: Reports Unit	2
BAGR, CD, Wright-Patterson AFB Attn: CADO-D1	1
OCSigO Attn: Ch. Eng. & Tech. Div., SIGTM-S	1
CG, AMC, Wright-Patterson AFB Attn: Eng. Div., Electronics Subdiv., MCREEO-2	1
CO, Air Force Cambridge Res. Labs., Attn: ERRS	1
CO, Watson Labs., AMC, Red Bank Attn: ENR	1
U. S. Atomic Energy Commission Attn: Mr. B. M. Fry	3
Office of Tech. Services, Dept. of Commerce	2
Dir., NBS, Washington, D. C. Attn: Dr. I. A. Dennison	1
RDB Attn: Library	2
Attn: Navy Secretary	1
Naval Res. Sec., Science Div., Library of Congress Attn: Mr. J. H. Heald	2

CONTENTS

Abstract	iv
Problem Status	iv
Authorization	iv
INTRODUCTION	1
Statement of the Problem	1
Known Facts Bearing on the Problem	1
EXPERIMENTAL METHOD	2
Instrumentation	2
Analysis of the Time-Potential Trace	5
Zinc-Steel Couple in Synthetic Sea Water	8
DATA AND EXPERIMENTAL RESULTS	11
Analysis of Time-Potential Traces	11
Electrode Potentials and Polarization of Zinc Anodes	11
Electrode Potentials and Polarization of Steel Cathodes	15
DISCUSSION AND CONCLUSIONS	21
General Theory	21
Zinc Anodes	24
Steel Cathodes	25
SUMMARY AND RECOMMENDATIONS	26
ACKNOWLEDGMENTS	26
REFERENCES	27

ABSTRACT

A d-c current interrupter method has been developed for oscilloscope studies of time-potential changes at an electrode surface during short interruption intervals. A square pulse with a very short rise time was used to interrupt the current flow in a cell. The current was cut off or on in 0.15 microsecond. The length of the interruption period and the pulse amplitude could be varied. The repetition rate of the interruption was adjusted so that the total interruption time was in the order of one percent of the current flow time.

This interrupter technique permitted correction for the resistance error in closed-circuit potential measurements. Polarization decay and build-up could also be followed as the current was cut off and turned on. The potential changes and double layer capacity effects occurring at an electrode surface during interruption could be measured. An initial study of polarization phenomena on the zinc anode-steel cathode system in a synthetic sea water electrolyte was carried out using this new interrupter method.

PROBLEM STATUS

This is an initial report; work on the problem is being continued.

AUTHORIZATION

NRL Problem C05-10R
NR 405-100

STUDIES OF TIME-POTENTIAL CHANGES ON AN ELECTRODE
SURFACE DURING CURRENT INTERRUPTION
PART I. ZINC-STEEL COUPLE IN SYNTHETIC SEA WATER

INTRODUCTION

Statement of the Problem

Several studies of the anodic behavior of zinc and aluminum-zinc alloys as protective anodes have been made at the Laboratory.^{1,2,3,4} These investigations demonstrated that high purity zinc was superior to other compositions studied for use in the cathodic protection of underwater steel structures on a ship.

In order to understand better the mechanism of this cathodic protection of steel by pure zinc anodes, it was felt that a fundamental study should be made of the polarization phenomena at anodic zinc and cathodic steel surfaces.

The study of polarization phenomena at an electrode surface requires the separation and determination of the various factors involved. When the closed circuit potential of a working electrode is measured, there is included in this measurement:

- (1) the IR drop due to resistance between the reference electrode and the double layer at the electrode surface;
- (2) a polarization voltage due to the voltage drop across the adsorbed double layer on the surface of the electrode; and
- (3) a polarization voltage due to the voltage drop across the diffuse double layer at the electrode surface.

Other factors may also affect the potential measured, but it is believed that the above three are the primary ones.

In order to measure these polarization factors, an electronic d-c current interrupter was devised. Corrosion cells consisting of pure zinc anodes and mild steel cathodes with a synthetic sea water⁵ electrolyte under constant current conditions were studied in this investigation.

Known Facts Bearing on the Problem

Many studies have been made of the polarization factors outlined above, and several techniques have been used for these investigations. This study involves the use of d-c transients. These d-c transients are produced by interrupting the flow of current in a cell

and studying the potential decay at the electrode surface. When the flow of current is again resumed, the build-up of potential can also be studied.

Two general methods used for the interruption of current flow are the commutator and the electronic interrupter methods. The commutator method has been extensively investigated by Newberry^{6,7,8} and Ferguson.^{9,10} An electronic interrupter method was devised by Hickling,¹¹ which allowed him to study potential decay during interruption of current from a minimum period of 10^{-5} second to a maximum period of 20×10^{-5} second. Hickling and Salt¹² later extended this range to a period of 10^{-1} second. By means of this electronic interrupter, the potential during current interruption was measured to an accuracy of 0.01 volt. The resistance error due to an IR drop between the reference electrode and the electrode surface was eliminated by measuring the potential at a sequence of increasing interruption intervals and then extrapolating back to zero time.

Frumkin¹³ criticized this extrapolation method for eliminating resistance error claiming that polarization decay in the order of 0.1 to 0.2 volt during the first 5×10^{-5} second was possible. In order to satisfy this criticism, Salt¹⁴ decreased the interruption time to the order of 2×10^{-6} second. However, this decrease of interruption time required a correction for what Salt refers to as a residual voltage, which for the shortest time interval was in the order of 0.75 volt.

In conjunction with a cathode-ray oscillograph, d-c transients can be used for the determination of the resistance error and study of the capacity effects at the electrode-solution interface. Bowden and Rideal¹⁵ used an oscillographic method to determine electrode capacities of metallic surfaces and by comparing with that of mercury claimed that they were able to determine the ratio: true area/apparent area. Newberry⁸ also used an oscilloscope in conjunction with his studies of hydrogen overvoltage decay during interruption of current.

The structure of the double layer at the surface of an electrode has been extensively investigated. A recent review of the studies on this subject has been made by Grahame.¹⁶ He defines the electrical double layer as possibly consisting of a layer of electrons, a layer of adsorbed ions, and a diffuse layer consisting of an ionic atmosphere in which ions of one sign are in excess of their normal concentration whereas those of the opposite sign are in concentrations lower than in the body of the solution. He pictured this atmosphere of abnormal concentration of ions to fall off rapidly as the distance from the surface increased. There also may exist at the interface a thin layer of neutral molecules.

EXPERIMENTAL METHOD

Instrumentation

The test equipment (Figures 1 and 2) consists of an interrupter circuit and a viewing circuit. The interrupter (Figure 3) produces a voltage pulse of variable amplitude and duration which is applied to the diode, T1, in such a fashion as to interrupt the current flowing in the circuit furnished by the battery, B1. The cell is connected in series with the battery, B1, a current limiting resistor, R1, a current measuring meter and the interrupter circuit. Two controls are furnished on the interrupter circuit. One control allows variable amplitudes of pulse to be applied to the diode so that a pulse amplitude just sufficient to interrupt the current may be chosen, and the other control allows the length of pulse applied to the diode to be varied. Pulse amplitudes up to 5 volts and pulse lengths from one to 120 microseconds are available. In order that the duty cycle of the interruption applied to the current passing through the cell shall not be varied, the repetition

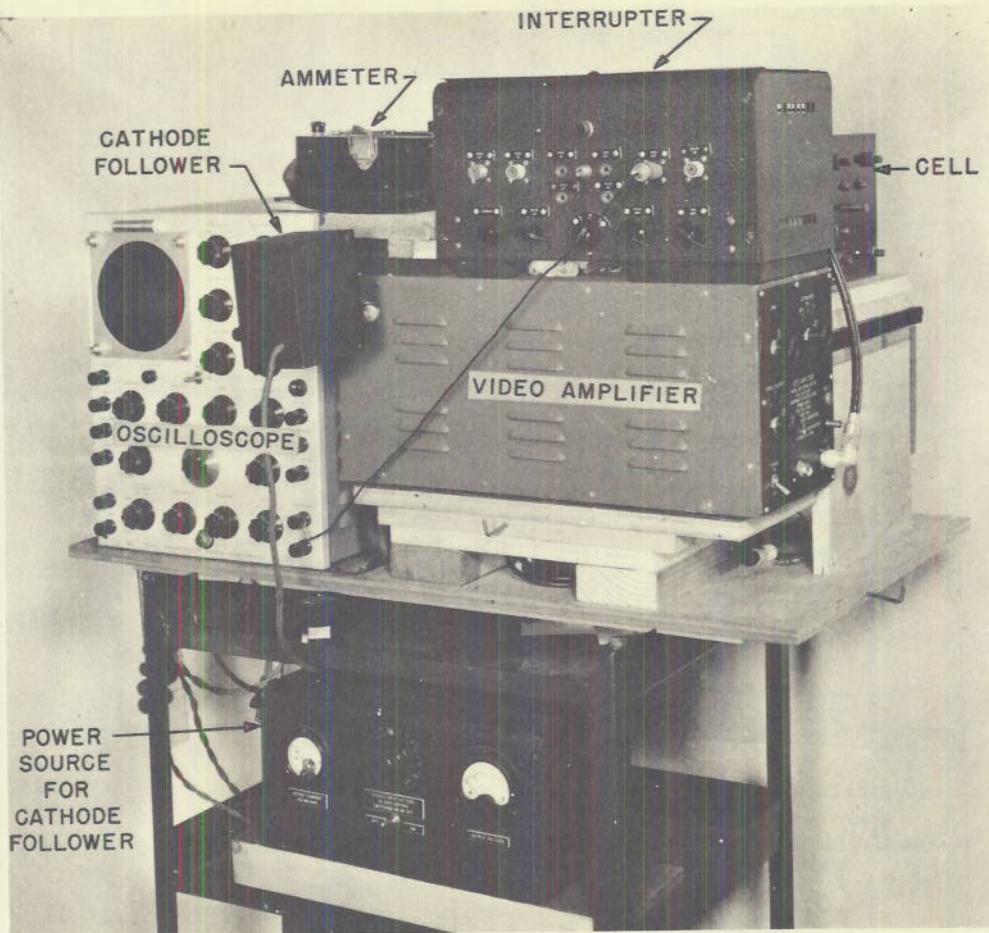


Figure 1 - Test equipment

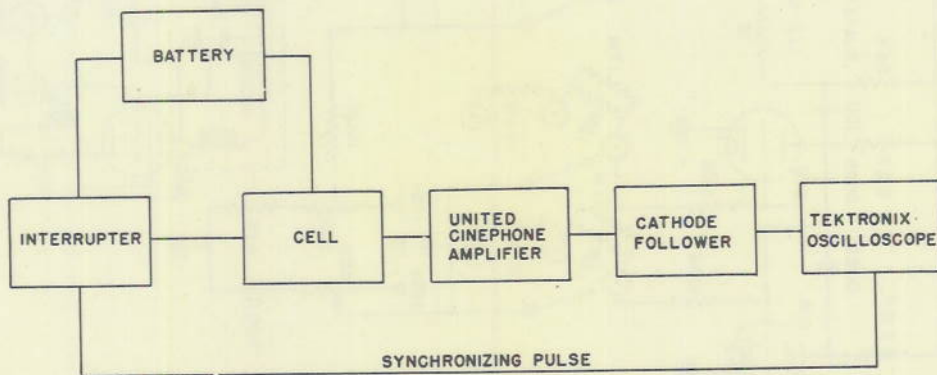
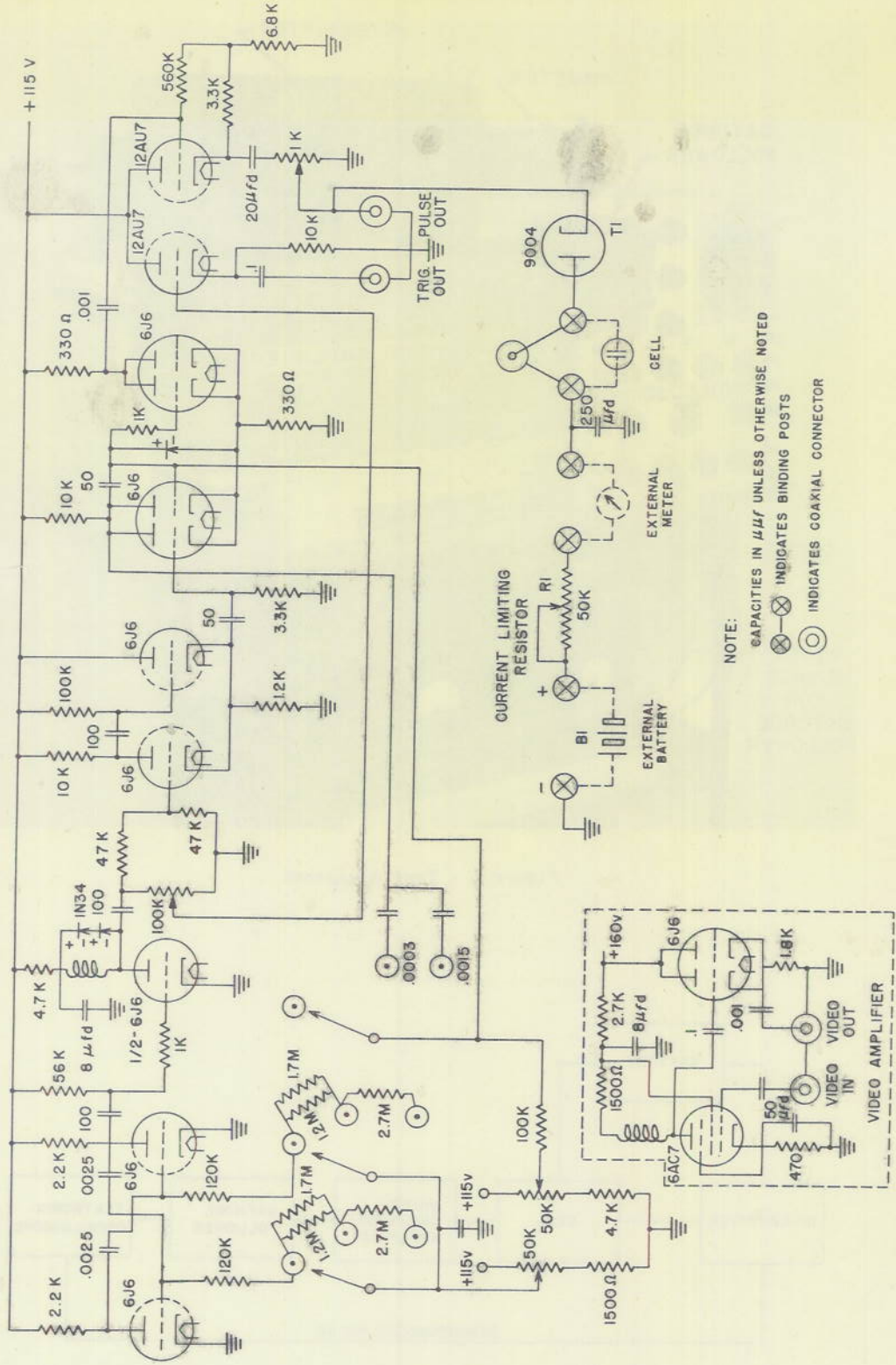


Figure 2 - Block diagram of test circuit



NOTE:
 CAPACITIES IN μfd UNLESS OTHERWISE NOTED
 ⊗ INDICATES BINDING POSTS
 ⊙ INDICATES COAXIAL CONNECTOR

Figure 3 - Interrupter circuit

rate of the pulse is varied by the same control as the pulse length in such fashion as to maintain the duty cycle constant at approximately one percent. The voltage pulse has a rise time from 0 to 90 percent of maximum amplitude of 0.08 microsecond and a fall time to 10 percent of maximum amplitude of 0.10 microsecond. No detectable overshoots are present and the pulse top is maintained flat over the entire range of variation of pulse lengths. A separate trigger pulse is also furnished by this circuit which serves to synchronize the external viewing scope.

The single stage video amplifier which is included in this unit has not been used in the experiments conducted here. The impedance offered by the cell to the flow of electric current is very low, on the order of 25 ohms, and with current of less than one milliampere this produces voltage drops of a few millivolts. To display the voltage pulse developed across the cell on an oscilloscope, an over-all amplification as high as 10,000 is sometimes required. Also, to pass the frequency components contained in the rise of this pulse, uniform gain response must be maintained up to four megacycles or better. In the test set-up employed here, this gain was provided by two video amplifiers in tandem. The first of these amplifiers is a high-gain amplifier built for the Naval Research Laboratory by the United Cinephone Company. This amplifier has a nominal response of 4 megacycles but at higher gain levels this response slopes off considerably at the high frequency end. The input impedance of this amplifier is 2.2 megohms shunted by 40 micromicrofarads which is sufficiently high to place a negligible load on the cell under measurement. The second amplifier is internal to the Tektronix oscilloscope, Type 511 AD, and has a nominal bandwidth of approximately 8 megacycles. The lack of required bandwidth on the United Cinephone amplifier shows up in two ways: (1) As a deterioration of the rise and fall times of the pulse, and (2) as an oscillation on the leading edge of the pulse. This effect becomes evident only when the waveform developed across the cell has a very sharp rise time (Figure 15, 1 microsecond interruption at 2 hours) and thus is usually encountered measuring the potential with respect to the cathode where the capacity effects are less pronounced.

The input impedance of the Tektronix oscilloscope is shunted by 40 micromicrofarads. If this capacitance were shunted across the high impedance output of the Cinephone amplifier a serious limitation of over-all bandwidth would occur. To avoid this a cathode follower impedance transformer (Figure 4) has been inserted between the output of the Cinephone amplifier and the input of the Tektronix oscilloscope.

The interrupter described here has been designed for a specific set of tests and does not indicate the range of pulse lengths and amplitudes possible. Should a requirement arise, pulses either much shorter or longer or of much greater amplitude could be obtained. It must be kept in mind, however, that reductions in pulse lengths with corresponding improvements in rise and fall times place severe requirements upon any amplifiers required.

Analysis of the Time-Potential Trace

In the study of the cathode-ray oscilloscope traces obtained during current interruption, it was helpful to consider the time-potential changes at an electrode surface in terms of an analogous electrical circuit. This circuit

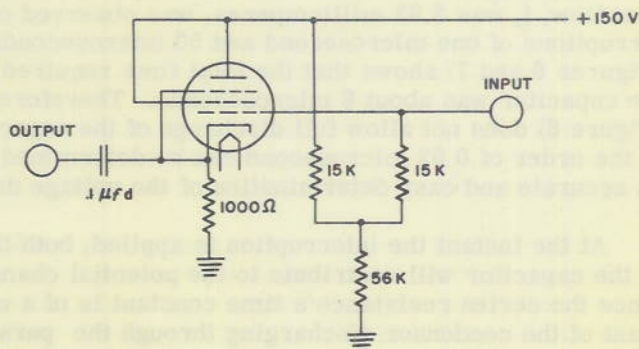


Figure 4 - Cathode follower circuit

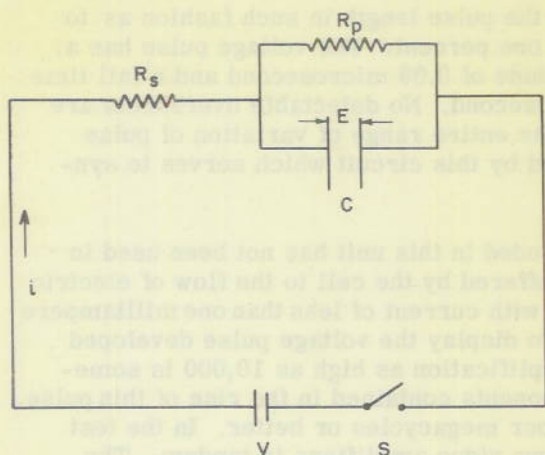


Figure 5 - Electrical analogy
of a time-potential trace

electrical condition at the electrode surface is more complex than during discharge. Here the series resistance, R_s , comes into the circuit and the change in voltage across the capacitor during charging will take place as shown by the following equation

$$E_C = E \left(\frac{R_p}{R_s + R_p} \right) \left(1 - e^{-\frac{t}{C} \left(\frac{1}{R_s} + \frac{1}{R_p} \right)} \right)$$

When the circuit (Figure 5) consists only of a resistance, the left hand side of the cathode ray trace (Figure 9) shows the drop in voltage across the resistance as the current is switched off, and the right hand side of the trace shows the increase in voltage as the current is turned on. The time constant of a pure resistance is undoubtedly of a much lower order than the time required for the switching off or on of the current. Therefore, the time required for voltage change across a pure resistance will only depend on the time necessary for the pulse to cut the current off and for the pulse to be cut off. This switching off and on of current for the interrupter circuit used took place in a time interval of 0.15 microsecond.

The potential change across a circuit (Figure 5) in which C was a 0.102 microfarad condenser, R_p a 20.8 ohm carbon resistor, R_s an 11.1 ohm carbon resistor, and the current flow, i , was 2.93 milliamperes, was observed on the oscilloscope during current interruptions of one microsecond and 50 microseconds. A study of the traces obtained (Figures 6 and 7) shows that the total time required for essentially complete discharge of the capacitor was about 6 microseconds. Therefore, the one-microsecond interruption (Figure 6) does not allow full discharge of the capacitor. However, since time intervals in the order of 0.02 microsecond can be determined, this short interruption time permits an accurate and easy determination of the voltage drop due to the series resistance.

At the instant the interruption is applied, both the series resistance and the discharge of the capacitor will contribute to the potential change observed in the trace. However, since the series resistance's time constant is of a much shorter order than the time constant of the condenser discharging through the parallel resistor, the voltage change during the first 0.15-microsecond interval will primarily consist of the change across the series resistance. The amount of capacitor voltage change during this first 0.15-microsecond

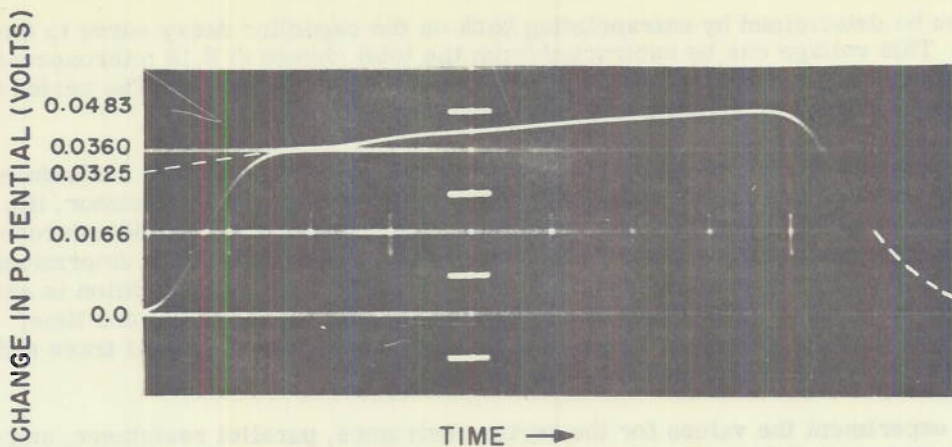
(Figure 5) consisted of a capacitor in parallel with a resistance and both of these in series with another resistance.

If the square pulse used to interrupt the current flow is considered as the switch, S , which cuts off the current, then, when S is opened the capacitor, C , will discharge through the parallel resistor, R_p . The equation for the change in voltage, E_C , across the capacitor during discharge when $R_p C$ is much greater than the rise time of the square pulse is

$$E_C = E e^{-t/R_p C},$$

where t is time and E is the voltage across the capacitor at t equal to zero.

When the interruption of current is ended, S is closed and current starts to flow. The



(EACH INTERVAL = 0.1 MICROSECONDS)

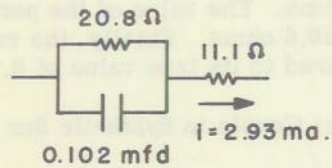
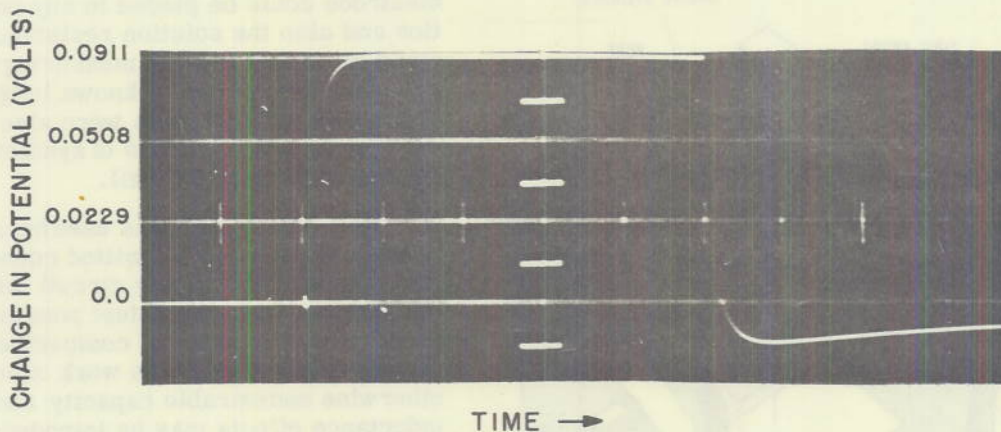


Figure 6 - Voltage change across circuit illustrated during a one-microsecond interruption



(EACH INTERVAL = 10 MICROSECONDS)

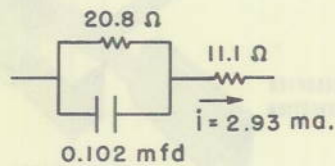


Figure 7 - Voltage change across circuit illustrated during a 50-microsecond interruption

interval can be determined by extrapolating back on the capacitor decay curve to the zero time axis. This voltage can be subtracted from the total change at 0.15 microsecond to give the voltage drop across the series resistance during current flow. The series resistance is determined by dividing the voltage drop by the current, i .

The time-potential trace (Figure 7) is used to determine the parallel resistance and the capacity values. The steady state voltage drop across the parallel resistor, $iR_p = E$ is determined by subtracting from the maximum voltage drop during the 50-microsecond interruption the voltage drop across the series resistor. The capacity is determined by finding the voltage E_C across the capacitor when $t = R_p C$. When this condition is satisfied, E_C will be equal to 0.368 times the voltage across the capacitor at zero time. The time when this value of voltage is reached is found from the time-potential trace and the capacity is determined by dividing this time by R_p .

In the experiment the values for the series resistance, parallel resistance, and capacity were determined from the traces (Figures 6 and 7) using the above method. The value of the series resistance was found to be 11.1 ohms as compared with the actual value of 11.1 ohms. The value of the parallel resistor was 20.0 ohms as compared to its true value of 20.8 ohms. Finally, the value determined for the capacitor was 0.108 microfarads as compared to its true value of 0.102 microfarads.

Zinc-Steel Couple in Synthetic Sea Water

A study of polarization phenomena at pure zinc anodes and mild steel cathodes was undertaken using the interrupter technique developed. Corrosion cells (Figure 8) used in these experiments consisted of lucite cylinders 10 centimeters in length. The ends of the cylinders were carefully machined to give smooth parallel surfaces. Ports were placed

in three positions so that a reference electrode could be placed in any position and also the solution resistance could be determined by measuring the potential drop across a known length of the cell. These ports were also used to allow a slow flow of synthetic sea water through the cell.

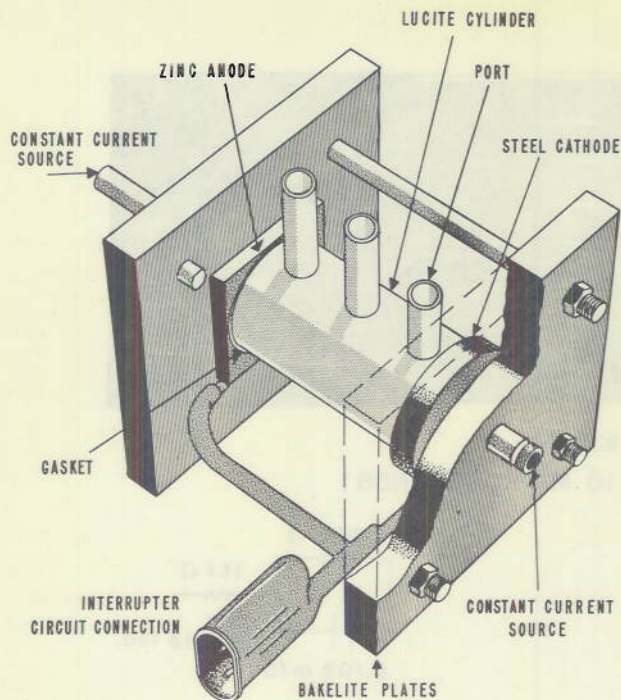


Figure 8 - Cell used in polarization studies

This type of cell was used because it was compact and permitted connection with the interrupter circuit with the shortest and straightest possible leads. Consideration of compactness is very important in this work since otherwise undesirable capacity and inductance effects may be introduced. The cylindrical type of cell also gives the optimum current distribution on both the electrodes and in the electrolyte, and permits a determination of solution resistance. Examination of the electrodes after a run readily revealed that edge effects were essentially eliminated by this cell.

The choice of reference electrode used in measuring the potential change

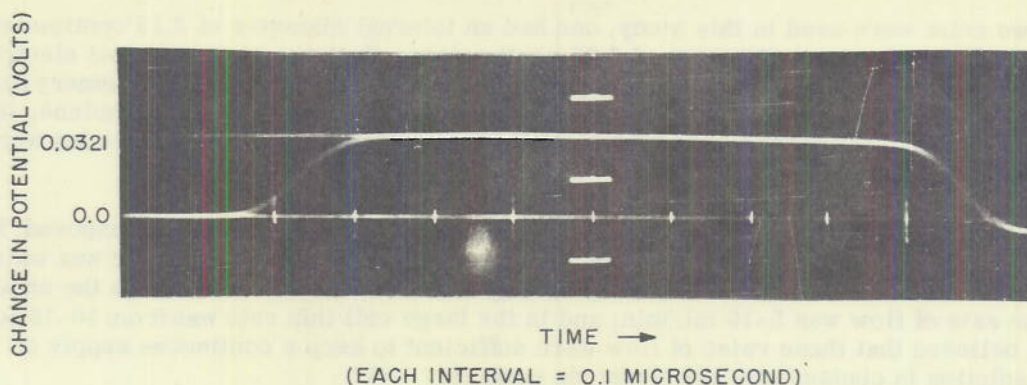


Figure 9 - Time-potential trace of voltage drop across cell due to solution resistance. One-microsecond interruption. Zinc reference electrodes

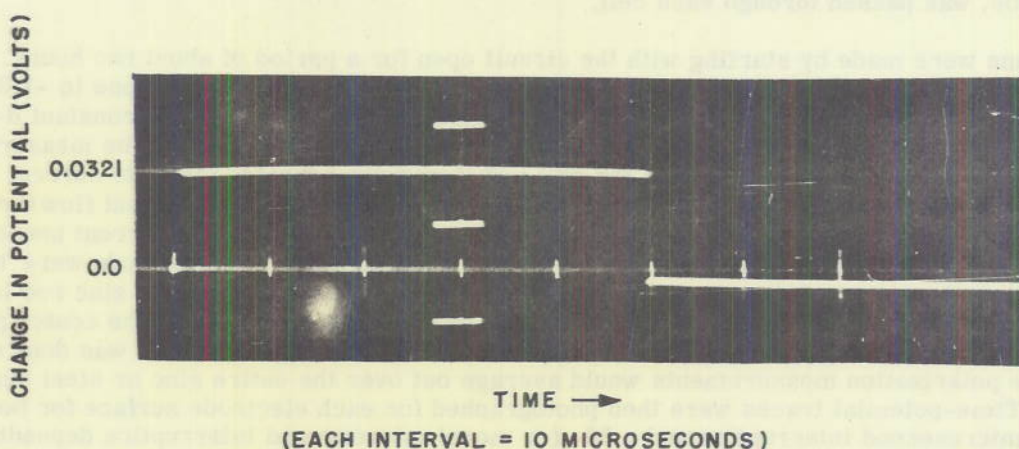


Figure 10 - Time-potential trace of voltage drop across cell due to solution resistance. 50-microsecond interruption. Zinc reference electrodes

during interruption was found to be critical. It was essential in the study of d-c transients at the electrode surfaces that the reference electrode remain constant during the interruption period and that it also have a very rapid response to voltage change. A saturated calomel reference electrode was first tried and was found to show a capacity effect. The reason for this is not fully understood and this phenomenon is to be further studied. However, it was found that a pure zinc or magnesium rod would make an ideal reference electrode for this work.

In order to test the suitability of pure zinc as reference electrodes, two zinc rods were inserted at the end port openings of a corrosion cell in the interrupter circuit. This was done so that each zinc rod would be at opposite ends of the potential field across the solution. These zinc rods were connected across the amplifier-oscilloscope circuit where the time-potential traces which were due to the IR drop in the solution between the two rods, were investigated. Traces for one- and 50-microsecond interruptions (Figures 9 and 10) show that the potential change during interruption was purely due to solution resistance and that the zinc rods themselves showed no discernible capacity effect or time lag in potential response.

Two cells were used in this study, one had an internal diameter of 3.18 centimeters; the other had an internal diameter of 6.35 centimeters. Both the zinc and steel electrodes were machined to a smooth surface and polished down to 3/0 metallographic emery paper. After cleaning the electrodes with water and ethyl alcohol, a gasket of polyethylene, one mil in thickness, was placed on the edges of the lucite cylinder and the electrodes were bolted into position (Figure 8).

In the small cell an apparent area of 7.94 sq cm of each electrode was exposed; for the large cell this area was 31.67 sq cm. A slow continuous flow of synthetic sea water which was saturated with air was passed through each cell during the run. In the small cell the rate of flow was 5-10 ml/min; and in the large cell this rate was from 10-15 ml/min. It was believed that these rates of flow were sufficient to keep a continuous supply of fresh solution in contact with the electrode surface.

During each run, closed circuit potentials against a saturated calomel reference electrode were continuously measured on a recording potentiometer. A continuous constant current, maintained by using a high voltage battery source across a voltage regulator vacuum tube, was passed through each cell.

Runs were made by starting with the circuit open for a period of about two hours. At this time the open circuit potentials of the zinc and steel were stable and close to -1.09 volts for the zinc and -0.75 volt for the steel electrodes. A predetermined constant d-c current was then applied to the cell. When the polarization factors were to be measured, the flow of sea water was stopped in the cell and it was disconnected from its current source. It was immediately connected to the interrupter circuit. The current flow through the interrupter circuit was maintained at the same value as the constant current source. Closed circuit potentials of each electrode using a saturated calomel electrode were then taken at each port opening. A pure zinc reference electrode consisting of a zinc rod long enough to extend almost to the bottom of the cell was then placed in either the center port opening or the opening farthest from the electrode being investigated. This was done so that the polarization measurements would average out over the entire zinc or steel surface. Time-potential traces were then photographed for each electrode surface for both a one-microsecond interruption and a 50- (or more) microsecond interruption depending on the time required for the polarization to decay to a steady value. The electrical connections across the reference electrode and the anode or cathode which were used to obtain the time-potential curves were made to the amplifier-oscilloscope circuit (Figure 11).

After the time-potential traces were photographed for each electrode surface, the closed circuit potentials at each port opening were then retaken with a saturated calomel electrode. The cell was then disconnected from the interrupter circuit and connected to its source of steady current. The oscilloscope was then calibrated for each amplifier setting used in the previous

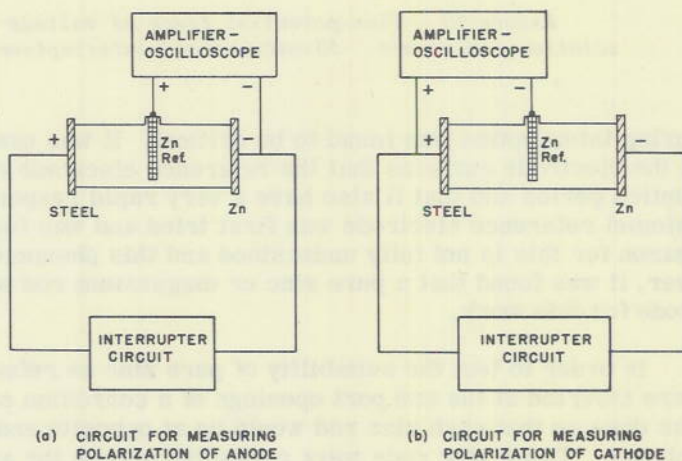


Figure 11 - Circuit arrangements used to obtain time-potential traces during interruption of current

measurements by taking the potential drop across a known carbon resistor in the interrupter circuit at known current values.

The duration of each run was from one to two weeks. Interrupter measurements were made at regular intervals during the run. There was no temperature control of the synthetic sea water electrolyte and it ranged from 24 degrees to 33 degrees C. The apparent current densities used were 0.1, 0.2 and 0.5 ma/sq cm for the small electrodes and 0.01, 0.05 and 0.1 ma/sq cm for the large electrodes.

At the end of each run the electrodes were examined. The steel cathodes in all cases had a uniform calciferous coating over the entire surface. A small amount of zinc metal precipitated at the bottom of the steel surface and was most noticeable for the higher current densities. There was no rust evident on the steel surfaces and after cleaning off the coating the steel was in practically the same condition as when new. The zinc electrodes were well pitted and the formation of a white coating was observed on all specimens. The zinc electrodes that were in the cells with the higher current densities were fairly evenly corroded; however, the anodes which were run at the lowest current densities showed large areas with no evident corrosion. There were relatively deep pits on these electrodes.

DATA AND EXPERIMENTAL RESULTS

Analysis of Time-Potential Traces

Time-potential traces showing potential change on the surface of an electrode during interruption were analyzed in the same way as for the circuit (Figure 5) previously described. This electrical analogy was assumed to hold for the potential changes taking place at the electrode surfaces during interruption. The series resistance was assumed to be the total resistance from the reference electrode to the double layer. This would include solution resistance plus resistance effects near the electrode surface due to concentration and other factors. The capacity effect was assumed to be due to one part of the double layer and the parallel resistance due to the resistance across that part of the double layer.

In order to show how the equations previously given for change in voltage across a capacity during discharge and charge fit the traces photographed, several typical ones are analyzed. The values determined for capacity, series and parallel resistance were substituted in the equations. The voltage across the capacity, E_C was then determined from these equations for various intervals of time. Original traces (Figures 12-14) of two typical time-potential curves for zinc anodes and one of a steel cathode were obtained. The time-potential points which were calculated from the discharge and charge equations were applied to the traces.

Electrode Potentials and Polarization of Zinc Anodes

The data obtained for the zinc anodes are shown in Table 1. The values for series resistance are primarily due to solution resistance. The reference electrode was not at all times the same distance from the zinc electrode, since in certain cases it was desirable to change this. Solution resistance was also determined by taking the potential change at various port openings in the cell. There was a definite indication that the series resistance was in general greater than could be accounted for by solution resistance measurements. This was probably due largely to the decrease in effective solution area at the double layer.

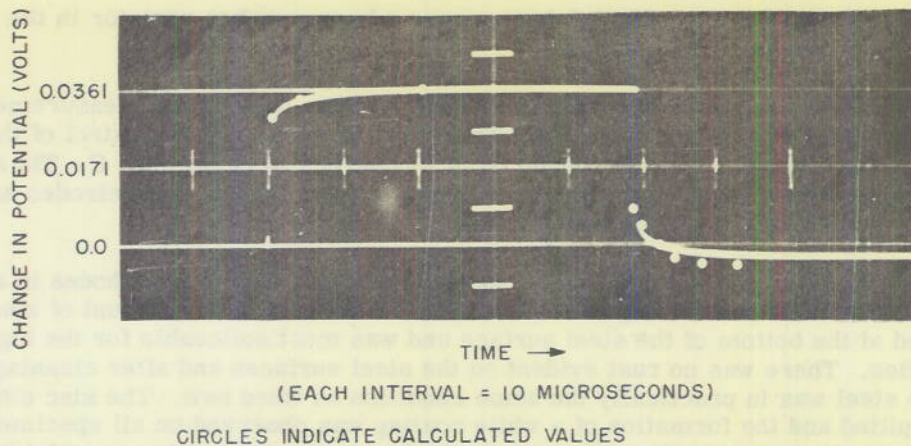


Figure 12 - Time-potential trace for zinc anode during current interruption. Small cell, apparent current density of 0.2 ma/sq cm after 237 hours

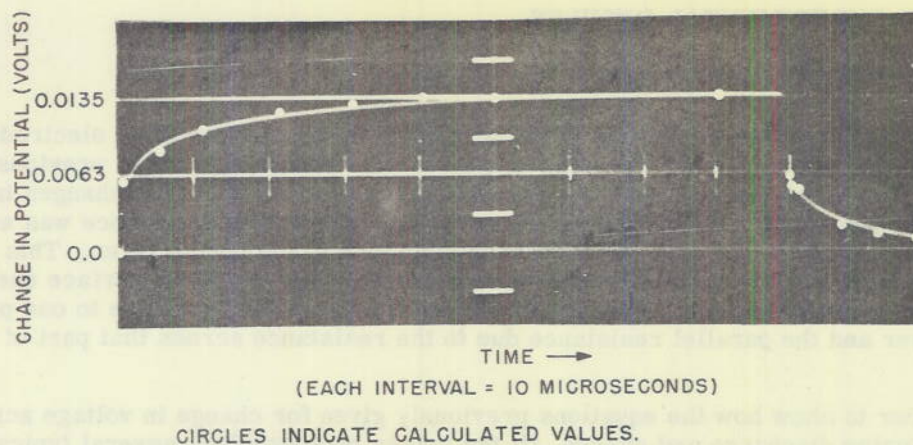


Figure 13 - Time-potential trace for zinc anode during current interruption. Large cell, apparent current density of 0.05 ma/sq cm after 169 hours

Figure 14 - Time-potential trace for steel cathode during current interruption. Small cell, apparent current density of 0.5 ma/sq cm after 237 hours

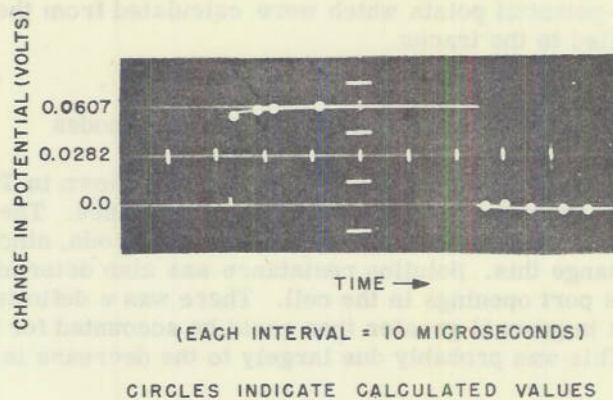


TABLE 1
Electrode Potentials and Polarization of Zinc Anodes

Apparent Area of Electrode (sq cm)	Apparent Current Density (ma/sq cm)	Duration of Run (hr)	Series Resistance, R_s (ohms)	Solution Resistance (ohms)	Parallel Resistance R_p (ohms)	Time Constant ($t=R_pC$) (10^{-3} sec)	Capacity Polarization E_C (v)	Capacity C (mfd)	Closed Circuit Potential (no series resistance) (v)	Residual Polarization (v)		
31.67	0.01	3	3.15	--	--	--	--	--	-1.090	0		
		27	5.05	--	1.26	3.64	0.0004	2.9	-1.040	0.050		
		51	5.05	--	1.58	7.7	0.0005	4.8	-1.028	0.061		
		71	5.05	--	1.89	--	0.0006	--	-1.015	0.074		
		146	5.36	--	2.20	20	0.0007	9.1	-1.004	0.085		
		170	4.42	--	3.79	--	0.0012	--	-0.999	0.090		
		191	8.20	--	6.31	--	0.0020	--	-0.994	0.094		
		214	4.73	--	6.00	14	0.0019	2.3	-0.983	0.095		
		240	4.73	--	5.36	14	0.0017	2.6	-0.993	0.095		
		31.67	0.05	3	2.28	2.85	--	--	--	--	-1.062	--
				23	3.04	2.65	1.08	7.7	0.0017	7.1	-1.017	0.071
				47	3.42	2.28	2.34	22.3	0.0037	9.5	-0.999	0.086
				70	3.35	2.59	3.35	15.0	0.0053	4.5	-0.995	0.090
				95	3.04	2.72	3.80	12.3	0.0060	3.2	-0.993	0.091
169	3.10			2.85	5.44	10.0	0.0086	1.8	-0.993	0.088		
192	3.04			2.53	5.63	9.6	0.0089	1.7	-0.992	0.089		
239	4.62			2.85	8.30	8.0	0.0131	1.0	-0.999	0.077		
31.67	0.05			4	4.24	4.45	0.25	0.5	0.0004	1.9	-1.075	0.015
				25	4.30	4.24	2.60	11.8	0.0041	4.6	-1.003	0.083
				49	4.81	4.37	2.98	11.8	0.0047	4.0	-1.001	0.084
				71	5.31	4.30	3.42	10.5	0.0054	3.1	-1.002	0.083
				100	4.94	4.24	4.05	10	0.0084	2.5	-1.001	0.083
				31.67	0.10	2	2.65	2.49	--	--	--	--
23	2.52	2.46	0.73			3.4	0.0023	4.7	-1.017	0.071		
46	2.68	2.24	1.92			11.35	0.0061	5.9	-1.000	0.084		
70	3.12	2.24	2.59			10.0	0.0082	3.9	-0.992	0.090		
95	3.00	2.43	3.98			6.6	0.0126	1.7	-0.987	0.090		

As can be seen in Table 1, the parallel resistance for each particular run generally increased with time. This is believed to be due to the decrease in area of the adsorbed double layer because of film build-up at the electrode surface.

The time constant, $t = R_p C$, generally decreased with time and as the apparent current density increased. Also the time constant for the large electrodes was of a higher order, even for the same apparent current density.

The capacity polarization for each run markedly increased with time due to the increase in parallel resistance. Increased current density also usually increased the capacity polarization.

The closed circuit potentials shown in Table 1 are the measured values against a saturated calomel electrode corrected for the IR drop due to series resistance. They, therefore, represent the polarization due to the adsorbed double layer plus the diffuse double layer plus any other possible polarization effects. The polarization due to what is believed to be the adsorbed double layer is the value E_C which is called the capacity polarization. The other polarization effects have been lumped together and called the residual polarization. This is obtained by taking the open circuit equilibrium value of potential for zinc, which is -1.09 volts in synthetic sea water and subtracting the closed circuit potential value plus the capacity polarization value. It is probable that this residual polarization is primarily due to concentration polarization effects. As can be seen from the table, this residual polarization for each run increases rapidly at first and after a few days levels off to a fairly constant value.

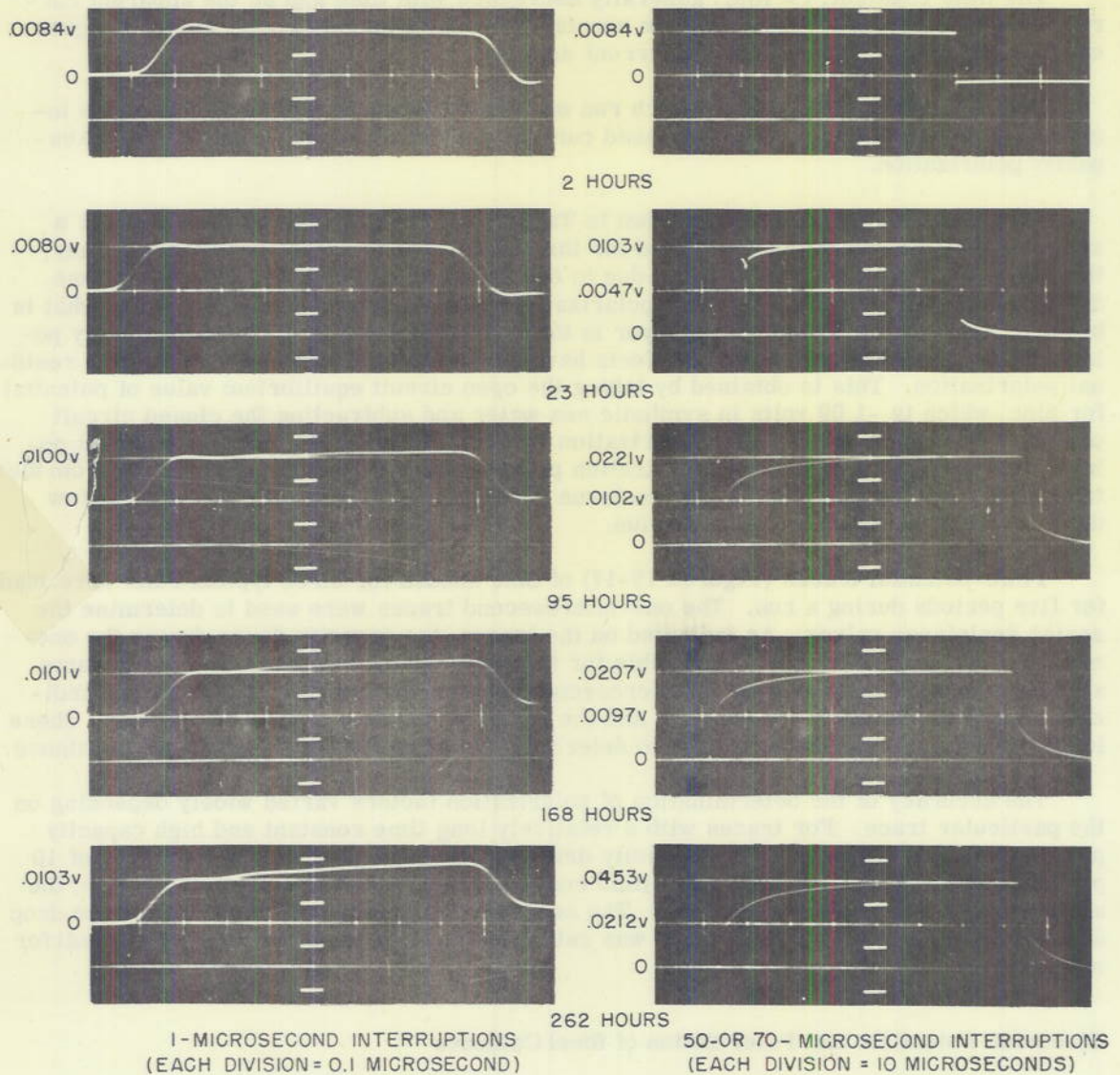
Time-potential traces (Figures 15-17) of zinc anodes for three typical runs were made for five periods during a run. The one-microsecond traces were used to determine the series resistance values. As indicated on the traces, the capacity decay during the one-microsecond interruption was negligible for the first day or two, after which it became significant. The longer 50- or 70-microsecond interruptions shown on the traces, indicate a marked change in the capacity and the parallel resistance effects with time. These longer traces, of course, were used to determine the capacity and the parallel resistance.

The accuracy of the determination of polarization factors varied widely depending on the particular trace. For traces with a relatively long time constant and high capacity polarization, the accuracy of the capacity determination was probably in the order of 10 percent. For traces with very short time constants and small capacity polarization, the accuracy was undoubtedly much less. The accuracy for determination of the voltage drop due to series and parallel resistance was estimated to be in the order of one millivolt for most cases.

Electrode Potentials and Polarization of Steel Cathodes

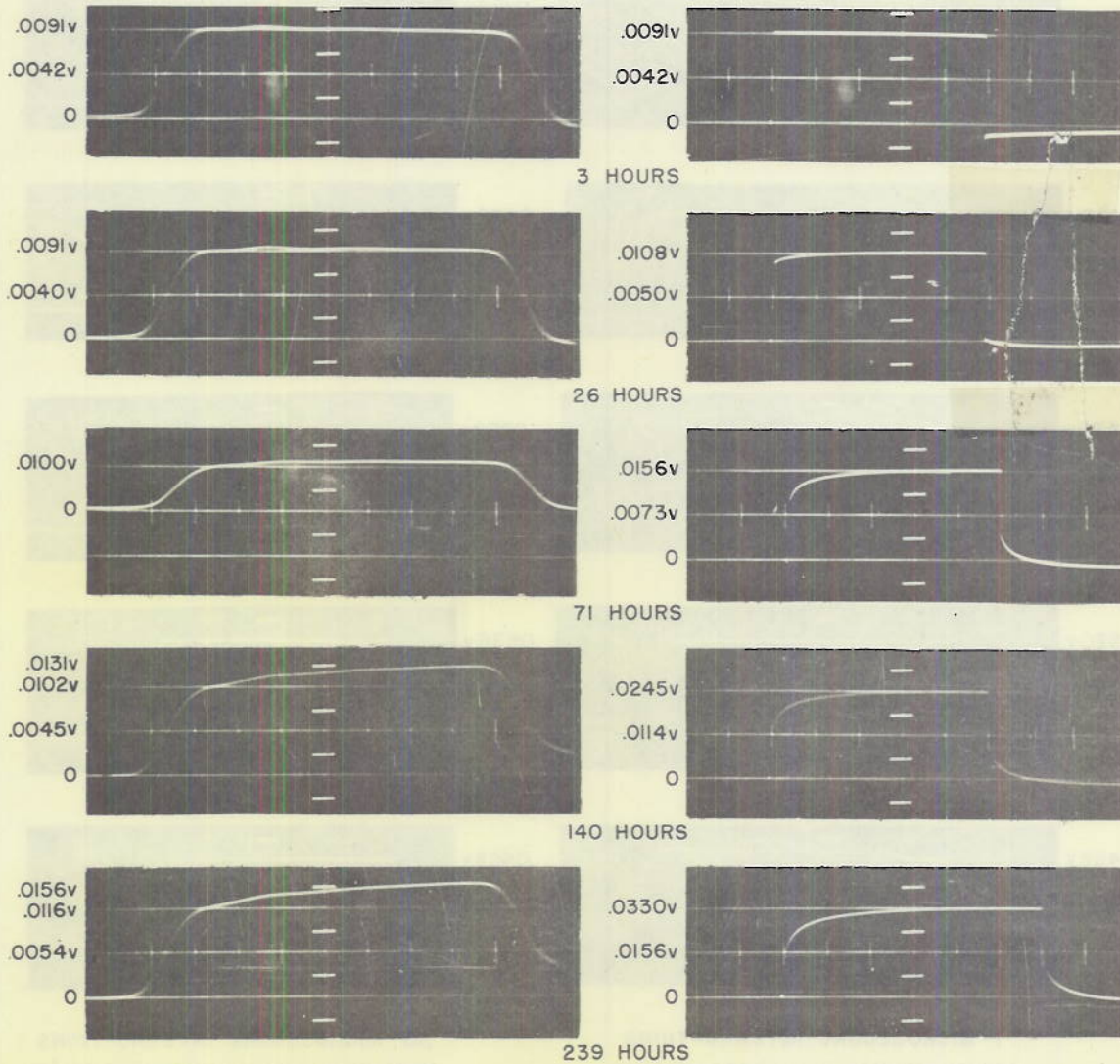
The time-potential traces for the steel cathodes were handled in the same manner as those for the zinc anodes. The capacity effects for steel cathodes under the experimental conditions used were not as marked as they were in the case of the zinc anodes and in many cases the capacity could not be determined with any degree of accuracy. The series resistance, however, could be determined in all cases and the closed circuit potential determined corrected for it. The parallel resistance was determined for all runs when it had a measurable effect during the maximum interruption time available.

Table 2 summarizes the measurements made for the steel cathodes. Here the series resistance as in the case of the zinc anodes, is also primarily due to solution resistance.



VERTICAL AXIS REPRESENTS VOLTAGE CHANGES DURING INTERRUPTION

Figure 15 - Time-potential traces of interruptions for 31.67 sq cm zinc anode at apparent current density of 0.1 ma/sq cm

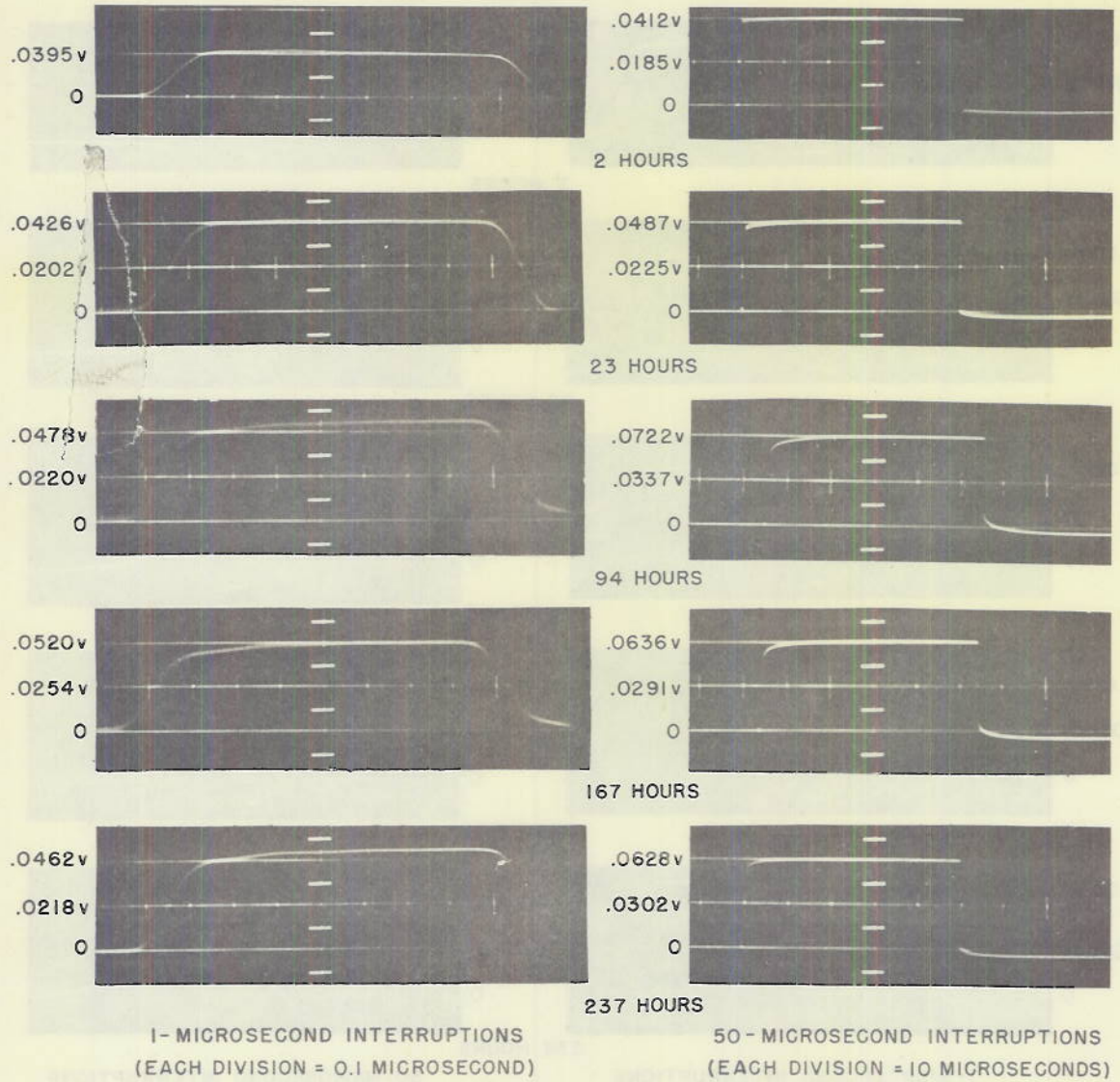


1- MICROSECOND INTERRUPTIONS
(EACH DIVISION = 0.1 MICROSECOND)

50-MICROSECOND INTERRUPTIONS
(EACH DIVISION = 10 MICROSECONDS)

VERTICAL AXIS REPRESENTS VOLTAGE CHANGES DURING INTERRUPTION

Figure 16 - Time-potential traces of interruptions for 7.94 sq cm zinc anode at apparent current density of 0.1 ma/sq cm



(VERTICAL AXIS REPRESENTS VOLTAGE CHANGES DURING INTERRUPTION)

Figure 17 - Time-potential traces of interruptions for 7.94 sq cm zinc anode at apparent current density of 0.5 ma/sq cm taken at intervals indicated

TABLE 2
Electrode Potentials and Polarization of Steel Cathodes

Apparent Area of Electrode (sq cm)	Apparent Current Density (ma./sq cm)	Duration of Run (hr)	Series Resistance, R_s (ohms)	Solution Resistance (ohms)	Parallel Resistance R_p (ohms)	Time Constant ($t-R_pC$) (10^{-6} sec)	Capacity Polarization E_C (v)	Capacity C (mid)	Closed Circuit Potential (no series resistance) (v)	Residual Polarization (v)	
31.67	0.01	3	5.05	--	--	--	--	--	-0.805	--	
		27	5.68	--	--	--	--	--	-0.841	--	
		51	5.36	--	--	--	--	--	-0.970	--	
		71	5.05	--	--	--	--	--	-0.996	--	
		146	4.73	--	--	--	--	--	-1.028	--	
		171	4.42	--	--	--	--	--	-1.062	--	
		191	8.20	--	--	--	--	--	-1.099	--	
		214	4.73	--	--	--	--	--	-1.115	--	
		240	5.99	--	--	--	--	--	-1.117	--	
		31.67	0.05	3	5.00	5.06	--	--	--	--	-1.019
23	4.81	4.81		--	--	--	--	--	-1.039	--	
47	5.25	4.12		--	--	--	--	--	-1.063	--	
70	4.62	4.67		0.51	0.0008	2	0.335	0.0008	-1.087	0.335	
95	4.94	4.87		--	--	--	--	--	-1.098	--	
169	5.19	5.06		0.95	0.0015	1.9	0.399	0.0015	-1.151	0.399	
192	5.06	4.55		1.27	0.0020	0.8	0.392	0.0020	-1.144	0.392	
239	5.44	5.06		1.39	0.0022	0.7	0.406	0.0022	-1.158	0.406	
31.67	0.05	4		3.98	4.43	--	--	--	--	-1.038	--
25		4.18		4.24	1.0	0.0016	0.7	0.341	0.0016	-1.093	0.341
49		5.00	4.37	0.70	0.0011	2.0	0.377	0.0011	-1.128	0.377	
71		5.00	4.30	1.1	0.0017	1.1	0.391	0.0017	-1.143	0.391	
100		4.94	4.24	1.1	0.0017	0.8	0.394	0.0017	-1.146	0.394	
31.67		0.10	2	2.59	2.49	--	--	--	--	-1.105	--
23			4.92	4.42	--	--	--	--	--	-1.165	--
46			4.73	4.07	--	--	--	--	--	-1.191	--
70			4.79	4.04	0.32	0.0010	2	0.462	0.0010	-1.213	0.462
95			4.76	4.32	0.32	0.0010	2	0.485	0.0010	-1.236	0.485
168	4.64		4.26	0.25	0.0008	2	0.493	0.0008	-1.244	0.493	
191	3.06		4.42	0.16	0.0005	3	0.500	0.0005	-1.253	0.500	
218	4.23		4.01	0.66	0.0021	1.4	0.500	0.0021	-1.252	0.500	
238	5.05		4.57	0.25	0.0008	3.6	0.521	0.0008	-1.272	0.521	
262	5.05		4.19	0.25	0.0008	3.6	0.522	0.0008	-1.273	0.522	

There was in several cases a marked increase in series resistance with time which was attributed primarily to a decrease in the effective area on the cathode surface because of film formation.

The parallel resistance and capacity polarization values were both of a lower order than for the zinc anodes and did not seem to vary as greatly with time.

The closed circuit potentials here are also corrected for series resistance and they represent the potential at the double layer. The residual polarization effects have been obtained by taking the open circuit equilibrium value of potential for steel in synthetic sea water of -0.75 volt and subtracting the closed circuit potential value minus the capacity polarization value. It is probable that residual polarization is mainly due to concentration polarization effects. As can be seen from Table 2, the residual polarization effects for the steel cathodes have been much higher and apparently more sensitive to current density than for the zinc anodes.

Time-potential traces of steel cathodes for a single run were made (Figure 18). The one-microsecond traces for the entire run indicated that there was an inappreciable amount of polarization decay during this interval and that this potential change was due to series resistance. The fifty-microsecond interruptions after the first day showed capacity effects which could be measured.

Since the changes occurring during interruption at the cathode surfaces were less pronounced than for the anode surfaces the accuracy in most cases of the measurements is less satisfactory.

DISCUSSION AND CONCLUSIONS

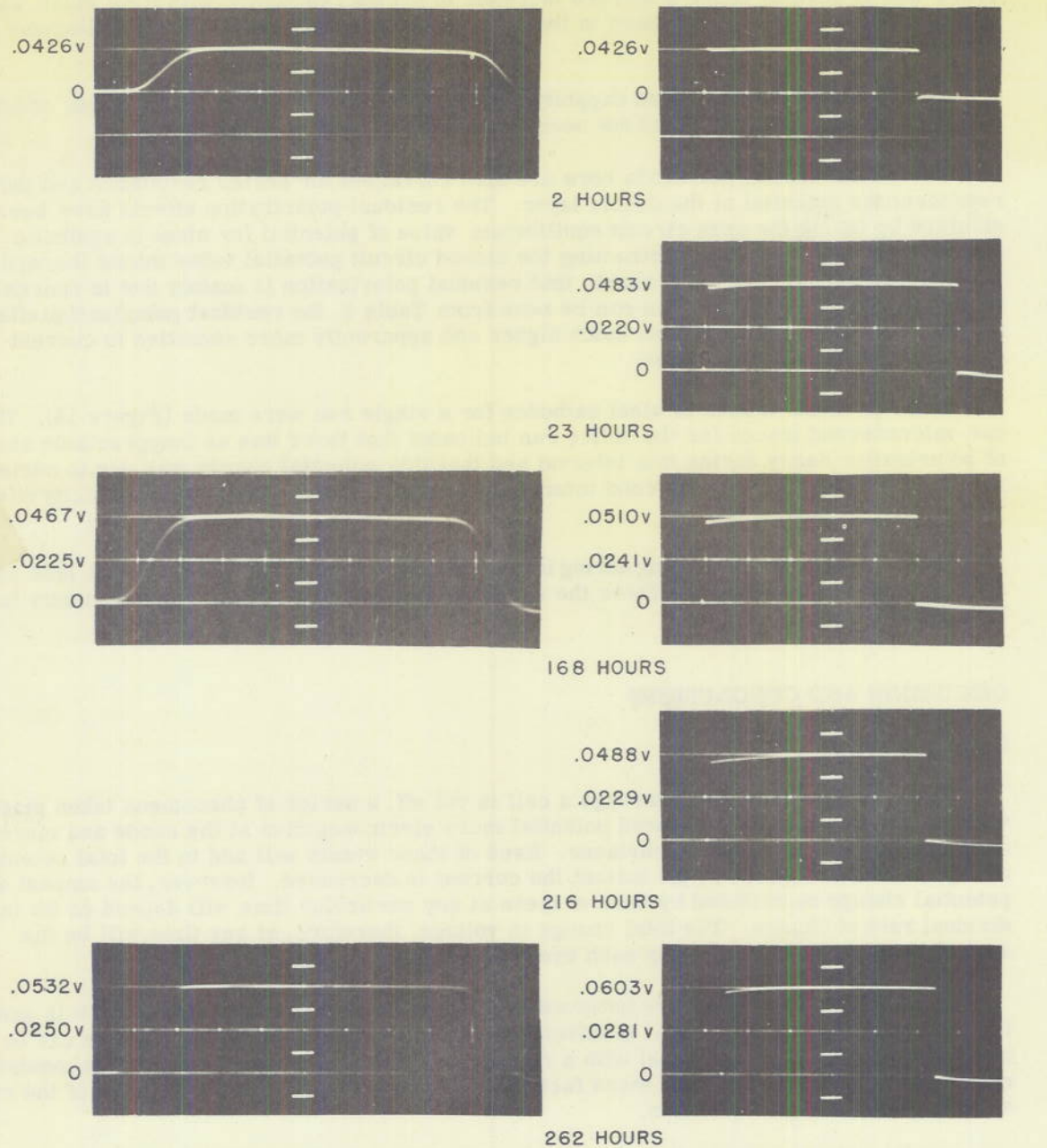
General Theory

When the current flowing through a cell is cut off, a series of phenomena takes place which tends to make the measured potential more electronegative at the anode and more electropositive at the cathode surfaces. Each of these events will add to the total potential change at each electrode at the instant the current is decreased. However, the amount of potential change contributed by each of these at any particular time will depend on its individual rate of change. The total change in voltage, therefore, at any time will be the sum of the potential changes for each event at that time.

At current cut-off there are believed to be three factors of major importance in causing potential change occurring at the electrode surface (Figure 19). Each of these can be considered a capacity in parallel with a resistance. Hence, an appropriate "time constant" can be attached to every one of these factors. This time constant is the product of the resistance and the capacity values.

The first of these factors is the IR drop due to the series resistance, R_s , between the reference electrode and the double layer at the electrode surface. The time constant for this event will be very short since the capacity attached to this resistance will be very small. As shown earlier in this paper the decay in potential due to this series resistance will take place within the time required for current cut-off, which for the experimental conditions used was in the order of 0.15×10^{-6} seconds.

The second factor, the voltage discharge, E_a , of the capacity due to the adsorbed double layer through its parallel resistance, R_a , undoubtedly will have a larger time constant than the series resistance; however, there may be some discharge during the cut-off



1-MICROSECOND INTERRUPTIONS
(EACH DIVISION = 0.1 MICROSECOND)

50-MICROSECOND INTERRUPTIONS
(EACH DIVISION = 10 MICROSECONDS)

(VERTICAL AXIS REPRESENTS VOLTAGE CHANGES DURING INTERRUPTION)

NOTE: 1-MICROSECOND INTERRUPTIONS AT 23 & 216 HOURS
NOT SHOWN BECAUSE THEY SHOWED NO CHANGE.

Figure 18 - Time-potential traces of interruptions for 7.94 sq cm steel cathode at apparent current density of 0.5 sq cm taken at intervals indicated

time. This polarization effect for all the cases encountered could easily be separated from the IR drop, due to series resistance, because the time constants of the former were appreciably greater in all runs than the cut-off time.

The third factor encountered in polarization measurements is the voltage drop, E_d , across the diffuse double layer. This is considered primarily a concentration effect, and it is evident that its time constant will also be larger than that of the series resistance.

There may be considerable overlapping between the three factors. This may consist of a diffuse double layer discharge with a time constant of the same order as the cut-off time and the adsorbed layer discharge. Or it may consist of an adsorbed double layer discharge which overlaps the diffuse double layer discharge time, both being considerably larger than the cut-off time. In interrupter studies of polarization phenomena, it is important, if possible, to arrange the experimental conditions so that the time constants of each of these three factors be as widely separated as possible.

Stern¹⁷ proposed the structure of the double layer outlined above. He combined the Helmholtz¹⁸ simple fixed adsorbed layer with the Gouy¹⁹ diffuse layer. If there is a total charge, q_T , on the electrode surface, then the corresponding charge in the electrolyte is made up of the adsorbed layer having a charge, $-q_a$, and the charge on the diffuse layer, q_d . Both q_a and q_d may have charges of the same or opposite sign but the condition

$$q_T = q_a + q_d,$$

is necessary when the system as a whole is electrically neutral.

Gatty and Spooner²⁰ from a study of the electrocapillary curve stated that close to the potential of the electrocapillary maximum the double layer is largely of the diffuse type. However, farther away from the potential of the electrocapillary maximum the capacity seemed constant over a considerable range of potential suggesting to them that the double layer is predominantly of the Helmholtz or adsorbed layer type.

Grahame^{16,21} assumes that the adsorbed double layer only contains such ions as may be specifically adsorbed on the metal surface. Since at the cathode specific cation adsorption can be considered negligible, each ion in the double layer will confer its own characteristic value of capacity on the adsorbed layer, the actual value being an average depending on the relative amounts of the several ions in the neighborhood of the adsorbed layer. Further, except near the electrocapillary maximum for very dilute solutions, the capacity of the adsorbed layer will be much smaller than the capacity of the diffuse layer.

Changes in concentration at the electrode surface result in concentration polarization phenomena. These concentration changes cause such occurrences as film formation, hydrogen liberation at the cathode, and liberation of oxygen at the anode. In addition to the diffuse

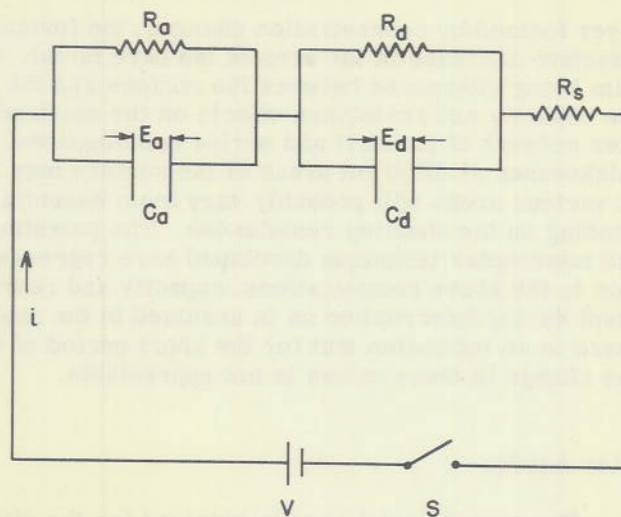


Figure 19 - Electrical analogy of the double layer at an electrode surface

layer formed by concentration changes, the formation of dielectric films may result in an effective decrease in the area of the bare metal. Capacity effects due to this dielectric film being interposed between the surface and the double layer will be present. Actually the capacity and resistance effects on the electrode surface must be looked upon as a complex network of parallel and series combinations. The dielectric constants and their thicknesses at different areas of the surface may vary greatly. Also the current density at various areas will probably vary from essentially zero to a relatively high value depending on the shunting resistances. The potential and capacity measurements made by the interrupter technique developed here represents an over-all average effect. In addition to the above complications, capacity and resistance values are not necessarily constant during interruption as is assumed in the analysis of the time-potential traces. However, there is an indication that for the short period of time required for these measurements the change in these values is not appreciable.

Zinc Anodes

The experimental results obtained for the zinc anodes indicated that for these runs the time constant for the capacity potential discharge was appreciably greater than the cut-off time. This permitted a good separation from potential drop due to series resistance. Since the total voltage drop due to polarization was not accounted for by the voltage drops across the capacity decay for the maximum interruption time available, it was evident that this polarization decay did not represent the total discharge of the double layer. Instead, it is believed that the adsorbed and the diffuse double layers had widely different time constants. The capacity discharge observed was for the section of the double layer having a time constant which allowed complete discharge during the interruption time used. The time constant of the remaining part of the double layer was of a much higher order and its discharge during this time was negligible.

It appears to be probable that the polarization decay observed at the zinc anodes is due to the discharge of the adsorbed double layer rather than that of the diffuse double layer. The capacity effect at the adsorbed double layer is due to a layer of adsorbed anions plus the concentration effects of neighboring ions in the diffuse layer. The adsorbed anions would react with the zinc ions going into solution, thus not allowing the capacity effect due to this specific adsorption of anions to build up to a high value. The formation of films due to the precipitation of the reaction products of zinc and the anions in the sea water would also tend to reduce the value of the adsorbed layer capacity because of the effective increase in dielectric thickness. The diffuse layer, however, will consist of a high concentration of positive zinc and other ions which should result in a high capacity value for this layer.

In the electrical analogy for the anode surface (Figure 19) the value of $C_a R_a$ is considered to be appreciably less than $C_d R_d$. There is virtually complete discharge of the adsorbed layer within the maximum interruption time available with the several possible exceptions which are shown in Table 1. For apparent current density values of 0.10 ma/cm^2 and below there was no measurable potential change in practically all runs until after the first day. The runs at higher current densities all showed relatively high capacities after the first several hours which dropped considerably the next day. The diffuse double layer discharge, however, apparently had a much larger time constant and its contribution to the potential change during interruption was negligible.

It was hoped that the capacity values found by this method could be used to determine the relative true current densities. The data, however, showed that there was no simple direct linear relationship between true area and capacity. The reason for this is believed

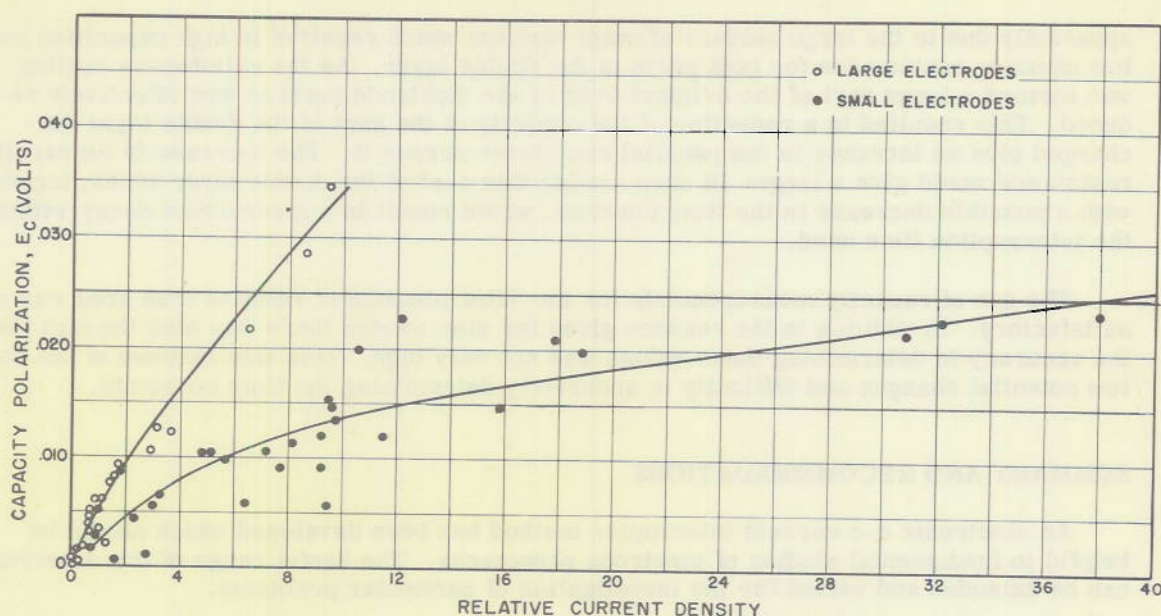


Figure 20 - Relationship between relative current density and capacity polarization of zinc anodes

to be mainly due to the fact that the capacitors formed by the adsorbed layer on the electrode surface are not flat plate condensers, because the contour of the surface is very irregular. The relative contour of the surface is also apparently not the same at different current densities or at different times during a run. There was, however, a fair relationship between area and capacity found for the large electrodes which were run at the lower current densities and the small electrodes run at the higher current densities, each taken as an individual group (Figure 20). The relative current density was calculated by assuming a direct linear relationship between area and capacity. The capacity value used as a base was the initial value found for the run at the highest apparent current density of 0.5 ma/sq cm. This was 14.8 microfarads and this value was divided by the apparent area of the electrode to give the relative area.

Steel Cathodes

The separation of the IR drop due to series resistance from the capacity voltage drop for the steel cathodes was easily accomplished since there were essentially no capacity voltage changes during the one-microsecond interruptions. The voltage change due to the capacity discharge was generally much smaller than for the zinc anodes and in many cases no potential change could be detected even at the maximum interruption time.

Table 2 shows that the measured capacity polarization was usually much less than one percent of the total polarization. Hence, the major polarization change did not take place since it apparently had a considerably higher time constant than 100 microseconds. It was not apparent in the case of steel cathodes whether the capacity effect observed consisted of the adsorbed or diffuse layer discharge.

Potential changes representing capacity discharge at the early part of the runs, especially at the lowest current densities used were negligible in most cases. This was

apparently due to the large surface of steel exposed which resulted in high capacities and low shunting resistances for both parts of the double layer. As the calciferous coating was formed a large part of the original area of the electrode surface was effectively reduced. This resulted in a reduction of the capacity of the part of the double layer discharged plus an increase in the parallel resistance across it. The increase in the parallel resistance would give a larger IR drop across this part of the double layer which, together with a possible decrease in the time constant, would result in a measurable decay within the interruption time used.

The use of capacity measurements for the determination of relative true area was not satisfactory. In addition to the reasons given for zinc anodes there was also the fact that the accuracy in determining these values was not very high. This was because of the very low potential changes and difficulty in accurately determining the time constants.

SUMMARY AND RECOMMENDATIONS

An electronic d-c current interrupter method has been developed which should be helpful in fundamental studies of electrode phenomena. The useful range of this interrupter can be extended and varied for the investigation of particular problems.

This electronic interrupter technique has been used to carry out a fundamental study of the zinc-steel couple in a synthetic sea water electrolyte. Series resistance effects in the measurement of closed circuit potentials have been eliminated. This method also permitted the placing of the reference electrode at a distance from the electrode being observed, thus eliminating local area effects and measuring the average potential on the electrode surface. This further resulted in more stable and, therefore, more accurate potential measurements.

The measurement of capacity effects due to the double layer and the polarization phenomena associated with these effects were carried out for the zinc and steel electrodes. This information should help to lead to a basic understanding of the electrochemical properties of these metals.

These investigations are preliminary; further studies of this type are necessary to give a more complete understanding of electrode processes.

The zinc-steel couple in a synthetic sea water electrolyte is a very complex system. Investigations of this couple in sea water should be supplemented by studies of more elementary systems. For example, the study of mercury as an electrode in simple salt, acid, and alkali electrolytes should be helpful in associating the measurements obtained by the interrupter method with the basic electrocapillary and double layer theories.

ACKNOWLEDGMENTS

The assistance of a number of the personnel of the Naval Research Laboratory was instrumental in carrying out this study. Thanks are due to Emmanuel Goldstein of the Optics Division for his suggestions on the use of pulses for current interruption; and to Neil Davis and Emerson Zettel of Radio Division III for their assistance and advice in the necessary electronic instrumentation.

* * *

REFERENCES

1. Gordon, G. S. "The Anodic Behavior of Zinc Alloys Used to Protect Steel in Sea Water." NRL Report P-2389, October 1944.
2. Gordon, G. S., Black, C. E., and May, T. P. "Second Report on the Anodic Behavior of Zinc Alloys Used to Protect Steel in Sea Water." NRL Report P-2592, July 1945.
3. May, T. P., Schuldiner, S., and Burbank, J. "The Anodic Behavior of Aluminum and Zinc Alloys in Sea Water." NRL Report C-3277, April 1948.
4. May, T. P., Gordon, G. S. and Schuldiner, S. "Anodic Behavior of Zinc and Aluminum-Zinc Alloys in Sea Water," "Cathodic Protection - A Symposium." p. 158, Houston, Texas: Electrochemical Society and National Association of Corrosion Engineers, 1949.
5. May, T. P., and Black, C. E. "Synthetic Ocean Water." NRL Report P-2909, August 1946.
6. Newberry, E. "The Life Period of the Overvoltage Compounds." J. Chem. Soc., 125: 511-518, 1924.
7. Newberry, E. "The Theory of Electrodes." Trans. Am. Electrochem. Soc., 58: 187-216, 1930.
8. Newberry, E. "Reversible Overvoltage." Trans. Faraday Soc., 43: 127, 1947.
9. Ferguson, A. L. "Polarization and Overvoltage with Special Attention Given to Transfer Resistance." Trans. Electrochem. Soc., 76: 113-143, 1939.
10. Ferguson, A. L., Discussions Faraday Soc., 1: 50, 1947.
11. Hickling, A. "Studies in Electrode Polarization, I." Trans. Faraday Soc., 33: 1540-1546, 1937.
12. Hickling, A., and Salt, F. W. "Studies in Hydrogen Overvoltage at High Current Densities, Part V." Trans. Faraday Soc., 37: 450-462, 1941.
13. Frumkin, A. "Contribution to the Theory of the Discharge of H Ions, Part I." Acta Physicochimica, URSS, 18: 23-57, 1943.
14. Salt, F. W., Discussions Faraday Soc., 1: 169, 1947.
15. Bowen, F. P., and Rideal, E. K. "The Electrolytic Behavior of Thin Films, Part I and Part II." Proc. Royal Soc., 120A: 59-79, 80-89, 1928.
16. Grahame, D. C. "The Electrical Double Layer and the Theory of Electrocapillarity." Chem. Reviews, 41: 441-501, 1947.
17. Stern, I., Z. Elektrochem., 30: 508, 1924.

18. von Helmholtz, H., *Gesamm. Abh.*, 1: 925, 1879.
19. Gouy, G. "Constitution of the Electric Charge at the Surface of an Electrolyte." *J. de Physique*, 9: 457-467, 1910.
20. Gatty, O., and Spooner, E. C. R. "The Electrode Behavior of Corroding Metals in Aqueous Solutions." p. 481, Oxford, Clarendon Press, 1938.
21. Grahame, D. C., "Properties of the Electrical Double Layer at a Mercury Surface II." *J. Am. Chem. Soc.*, 68: 301-310, 1946.

* * *